
Variational Classification

Shehzaad Dhuliawala¹ Mrinmaya Sachan¹ Carl Allen^{1,2}

Abstract

We present a novel extension of the traditional neural network approach to classification tasks, referred to as variational classification (VC). By incorporating latent variable modeling, akin to the relationship between variational autoencoders and traditional autoencoders, we derive a training objective based on the evidence lower bound (ELBO), optimized using an adversarial approach. Our VC model allows for more flexibility in design choices, in particular class-conditional latent priors, in place of the implicit assumptions made in off-the-shelf softmax classifiers. Empirical evaluation on image and text classification datasets demonstrates the effectiveness of our approach in terms of maintaining prediction accuracy while improving other desirable properties such as calibration and adversarial robustness, even when applied to out-of-domain data.

1. Introduction

Classification is a core task in machine learning, used to categorise objects (Klasson et al., 2019), provide medical diagnoses (Adem et al., 2019; Mirbabaie et al., 2021) or identify potentially life-supporting planets (Tiensuu et al., 2019). Classification also arises in other learning paradigms, e.g. to select actions in reinforcement learning or distinguish positive and negative samples in contrastive learning, and is related to the *attention* mechanism in large language models. It is common to tackle classification tasks with domain-specific neural networks with a *sigmoid* or *softmax* output layer.¹ A network f_ω , with weights ω , deterministically maps each data point x (in a domain \mathcal{X}) to a real vector $z = f_\omega(x)$ that is then transformed in the output layer to a point on the simplex $\Delta^{|\mathcal{Y}|}$, the parameter of a discrete distribution $p_\theta(y|x)$ over class labels $y \in \mathcal{Y}$:

$$p_\theta(y|x) = \frac{\exp\{z^\top w_y + b_y\}}{\sum_{y' \in \mathcal{Y}} \exp\{z^\top w_{y'} + b_{y'}\}}. \quad (1)$$

While softmax classifiers often outperform alternatives and are an attractive option, their inner workings are not well

¹Since the softmax function generalises the sigmoid to multiple classes, we refer to softmax throughout, but arguments also apply to the sigmoid case.

understood theoretically and they are not without issue. The overall mapping from \mathcal{X} to $\Delta^{|\mathcal{Y}|}$ is learned numerically by minimising a loss function over finite training samples, the result of which is in many respects a “black box”, making predictions that are hard to explain. Neural networks are typically highly flexible, so that the model $p_\theta(y|x)$ can approximate the true data distribution $p(y|x)$, but, the function class $\{f_\omega\}_{\omega \in \Omega}$ may contain many functions (for different ω) that achieve similar accuracy over the training set, but elsewhere give differing and hence *uncertain* predictions. Other known issues include *adversarial examples*, where predictions erroneously vary for imperceptible changes in the data; and *miscalibration*, where output class-conditional probabilities poorly reflect the uncertainty of a class.

Looking to address the shortcomings of softmax classification generally, we investigate the underlying predictive mechanism from a latent variable perspective. We treat z of Equation 1 as a latent variable and consider the (Markov) generative process $y \rightarrow z \rightarrow x$. It is desirable if a classifier can learn to reverse the true generative process and stochastically map data samples x to their respective latent variables z , since the latent representations then capture semantic and probabilistic information of the data, and the mapping $x \rightarrow z$ may need to learn salient features of the data to achieve that.

A *variational classifier* (VC) explicitly reverses the generative model, with class predictions given by $p_\theta(y|x) = \int_z p_\theta(y|z)p_\theta(z|x)$. $p_\theta(z|x)$ is assumed to be parameterised by a neural network f_ω , and $p_\theta(y|z) = \frac{p_\theta(z|y)p_\pi(y)}{\sum p_\theta(z|y')p_\pi(y')}$ is defined by class-conditional priors $p_\theta(z|y)$ and Bayes’ rule. Parameters of a VC can be trained under an analogue of the evidence lower bound (ELBO) used to train a variational auto-encoder (VAE) to model $p_\theta(x) = \int_z p_\theta(x|z)p_\theta(z)$ (Kingma & Welling, 2014). We show that softmax cross entropy (SCE) loss is a special case of this ELBO-analogue. This is instructive as it reveals that, in general, a softmax classifier *does not reverse the generative process* to learn latent structure, even though class predictions, given by $p_\theta(y|z)$, may assume specific class-conditional structure $p_\theta(z|y)$.

Indeed, in practice, the SCE loss may be minimised by “collapsing” the *empirical* distribution of latent variables for a class y , defined by passing class samples through the neural network $\{z = f_\omega(x); x \sim p(x|y)\}$, to a point. In short,

a softmax classifier can learn to classify without learning meaningful latent structure.

Based on this, we introduce a regularisation term to encourage the empirical class-conditional latent distributions to fit the expected class priors $p_\theta(z|y)$. Specifically, we minimise a Kullback-Leibler (KL) divergence between these two approximations to $p(z|y)$, which is non-trivial since the empirical distribution can only be sampled from. As seen elsewhere (Gutmann & Hyvärinen, 2010; Makhzani et al., 2015; Mescheder et al., 2017), we take an *adversarial* approach to implicitly learn log ratios of the distributions.

The resulting variational classifier generalises the typical softmax classifier from a latent perspective, while the training regime also fits the distribution of latent variables to chosen class priors $p_\theta(z|y)$. Within the VC framework, the latent variables learned by a softmax classifier can be considered *maximum likelihood* point estimates, maximising $p_\theta(y|z)$. The KL divergence of the VC objective introduces two terms: class priors, which alone would give *maximum a posteriori* latent point estimates; and entropy that encourages latent variables to *fit* rather than maximise the class priors, a more *Bayesian* approach (see Figure 2). We note that terms of the standard ELBO can be interpreted similarly.

Variational Classification is designed to give a classifier that better reflects the (inverted) data generative process. A VC is not necessarily expected to classify more accurately than a softmax classifier given sufficient data, since the constraints in latent space compensate for sampling noise, but the improved latent structure is anticipated to holistically improve a softmax classifier in low data regimes, and in other respects by capturing more information in the data. Through a series of experiments in vision and text domains, we demonstrate that a VC indeed achieves comparable classification accuracy to regular softmax while outperforming in terms of calibration, robustness to adversarial perturbations, performance in low data regimes and generalisation under domain shift. We note that many methods have been proposed to address a particular issue of softmax classification, such as calibration or adversarial robustness, which typically require issue-specific hyperparameters to be tuned, whereas we seek to address all issues simultaneously without any issue-specific hyperparameters of validation set.

The VC framework offers fundamental mathematical insight into softmax classification, increasing its interpretability and opening it up to potential principled improvement and integration with other latent variable methods, such as VAEs or contrastive learning.

2. Background (Variational Auto-Encoder)

The generalisation of softmax to variational classification is analogous to how a deterministic auto-encoder relates to a

variational auto-encoder, which we briefly summarise.

Estimating parameters of the latent variable model $p_\theta(x) = \int_z p_\theta(x|z)p_\theta(z)$ by maximising the data likelihood is intractable in general, instead the *evidence lower bound* (ELBO) is maximised:

$$\begin{aligned} & \int_x p(x) \log p_\theta(x) \\ &= \int_x p(x) \int_z q_\phi(z|x) \left\{ \log p_\theta(x|z) - \log \frac{q_\phi(z|x)}{p_\theta(z)} + \log \frac{q_\phi(z|x)}{p_\theta(z|x)} \right\} \\ &\geq \int_x p(x) \int_z q_\phi(z|x) \left\{ \log p_\theta(x|z) - \log \frac{q_\phi(z|x)}{p_\theta(z)} \right\} \doteq \text{ELBO} \end{aligned} \quad (2)$$

Maximising the ELBO is equivalent to minimising

$$D_{\text{KL}}[p(x) \parallel p_\theta(x)] + \mathbb{E}_x [D_{\text{KL}}[q_\phi(z|x) \parallel p_\theta(z|x)]], \quad (3)$$

where $D_{\text{KL}}[p(x) \parallel q(x)] = \int_x p(x) \log \frac{p(x)}{q(x)}$ is the Kullback-Leibler (KL) divergence. This shows that maximising the ELBO fits the model $p_\theta(x)$ to the data distribution $p(x)$ while also fitting the approximate posterior $q_\phi(z|x)$ to the model posterior $p_\theta(z|x) = \frac{p_\theta(x|z)p_\theta(z)}{p_\theta(x)}$, encouraging the two modelled distributions, $q_\phi(z|x)$ and $p_\theta(x|z)$, to be *consistent under Bayes' rule*.

The variational auto-encoder (VAE) (Kingma & Welling, 2014; Rezende et al., 2014) is an implementation of the ELBO in which all distributions are assumed Gaussian, and $p_\theta(x|z)$, $q_\phi(z|x)$ are parameterised by neural networks. If the variance of q_ϕ tends to zero, q_ϕ tends to a delta distribution and the first (“reconstruction”) term of Equation 2 tends to the loss function of a deterministic auto-encoder. Hence, the VAE can be seen to generalise the deterministic case, allowing for uncertainty or stochasticity in the latent z , while also constraining its marginal distribution $p(z)$ through the second (“regularisation”) term.

3. Variational Classification

A typical softmax classifier is a deterministic function that maps each data point $x \in \mathcal{X}$ through a sequence of intermediate representations to a point on the simplex $\Delta^{|\mathcal{Y}|}$ that parameterises a predicted categorical distribution $p_\theta(y|x)$ over labels $y \in \mathcal{Y}$. We treat x, y as samples of random variables x, y from a joint distribution $p(x, y)$. An intermediate representation $z = g(x)$ can be treated similarly as a *latent* random variable z sampled from $p(z|x) = \delta_{z-g(x)}$, a delta distribution.

Generalising this, a **variational classifier** (VC) assumes the generative Markov model $y \rightarrow z \rightarrow x$, with predictions defined in the reverse direction:

$$p_\theta(y|x) = \int_z p_\theta(y|z)p_\theta(z|x), \quad (4)$$

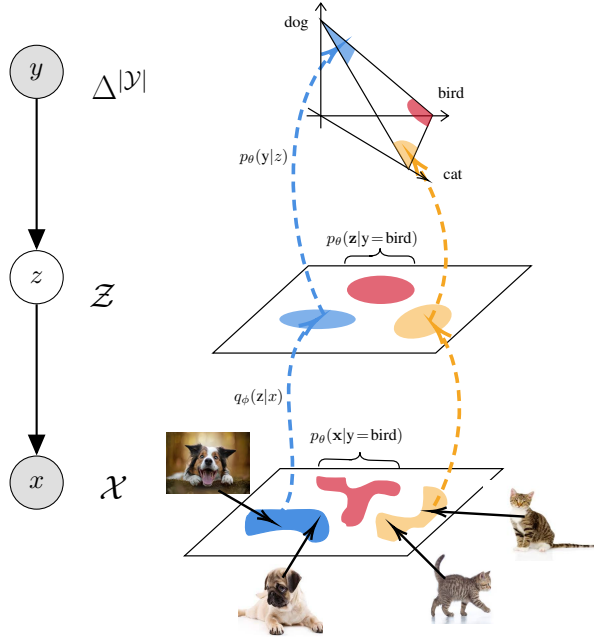


Figure 1: The Variational Classifier: reversing the generative process; $q_\phi(z|x)$ stochastically maps data $x \in \mathcal{X}$ to the latent space \mathcal{Z} , where *empirical* latent distributions $q_\phi(z|y) \doteq \int q_\phi(z|y)p(x|y)$ are fitted to *class priors* $p_\theta(z|y)$; the output layer computes class predictions $p_\theta(y|z)$ by Bayes' rule.

and $p_\theta(z|x)$ parameterised by a neural network $f_\omega: \mathcal{X} \rightarrow \mathcal{Z}$ (see Fig. 1). A softmax classifier can be seen as a specific case of Equation 4, where the input to the softmax layer is considered the latent variable z ; $p_\theta(z|x) = \delta_{z-f_\omega(x)}$, a delta distribution parameterised by the neural network up to the softmax layer; and $p_\theta(y|z)$ is defined by the softmax layer.

As with the latent variable model for $p_\theta(x)$ (§2), parameters of a VC cannot generally be learned by maximising the likelihood, but a lower bound is given (*cf* Eq. 2) by:

$$\begin{aligned} & \int_{x,y} p(x,y) \log p_\theta(y|x) \\ &= \int_{x,y} p(x,y) \int_z q_\phi(z|x) \left\{ \log p_\theta(y|z, \textcolor{red}{x}) - \log \frac{q_\phi(z|x)}{p_\theta(z|x)} \right. \\ & \quad \left. + \log \frac{q_\phi(z|x)}{p_\theta(z|x,y)} \right\} \\ & \geq \int_{x,y} p(x,y) \int_z q_\phi(z|x) \log p_\theta(y|z) \doteq \mathbf{ELBO}_{\mathbf{VC}}, \end{aligned} \quad (5)$$

where $p_\theta(y|z, x) = p_\theta(y|z)$ (by Markov); and the variational posterior q_ϕ is chosen to depend only on x and set numerically equal to $p_\theta(z|x)$ (eliminating the second term, line 2).² Unlike in the standard ELBO, the KL term $D_{\text{KL}}[q_\phi(z|x) \parallel p_\theta(z|x,y)]$, minimised implicitly when maximising $\mathbf{ELBO}_{\mathbf{VC}}$, may not reach zero in general, only in the limiting case when $p_\theta(y|x, z) = p_\theta(y|z)$ and z is a *sufficient statistic* for y given x , i.e. z contains all information about y

²As such, “ $p_\theta(z|x)$ ” and “ $q_\phi(z|x)$ ” are interchangeable, but we use the latter since $q_\phi(z|y)$ is then labelled intuitively and distinguished from $p_\theta(z|y)$, a different model of that distribution.

in x .³ Hence maximising $\mathbf{ELBO}_{\mathbf{VC}}$ implicitly encourages z towards a sufficient statistic. Cross-entropy loss is a special case of $\mathbf{ELBO}_{\mathbf{VC}}$ where $q_\phi(z|x) = \delta_{z-f_\omega(x)}$, hence softmax cross-entropy loss is a special case of $\mathbf{ELBO}_{\mathbf{VC}}$:

$$\begin{aligned} & \int_{x,y} p(x,y) \int_z q_\phi(z|x) \log p_\theta(y|z) \stackrel{q=\delta}{=} \int_{x,y} p(x,y) \log p_\theta(y|z=f_\omega(x)) \\ &= \int_{x,y} p(x,y) \log \frac{\exp\{f_\omega(x)^\top w_y + b_y\}}{\sum_{y'} \exp\{f_\omega(x)^\top w_{y'} + b_{y'}\}}, \end{aligned} \quad (6)$$

in which $p_\theta(y|z) = \frac{p_\theta(z|y)p_\theta(y)}{\sum_{y'} p_\theta(z|y')p_\theta(y')}$ implicitly assumes $p_\theta(z|y) \propto \exp\{z^\top w_y + b_y\}$, $\forall y \in \mathcal{Y}$, equal-scale exponential family forms (absorbing $\log p(y)$ into constant b_y).

This shows that for softmax classification to reliably output label distributions, latents z should follow specific class-conditional distributions, or “class priors”, $p_\theta(z|y)$. However, the *empirical* distribution of $z|y$ is defined by $q_\phi(z|y) \doteq \int_x q_\phi(z|x)p(x|y)$, i.e. by the outputs of the neural network f_ω given samples x of class y . The question then is: do these two versions of the same distribution, $p_\theta(z|y)$ and $q_\phi(z|y)$, match? The answer to which is determined by $q_\phi(z|x)$ that maximises $\mathbf{ELBO}_{\mathbf{VC}}$. In general, this is given by $q_\phi(z|x) = \delta_{z-z_x}$, where $z_x = \arg \max_z \sum_y p(y|x) \log p_\theta(y|z)$ (see §A.1 for a proof). In practice, $p(y|x)$ is not known, we only have samples from it. In a continuous data domain \mathcal{X} , the same x is resampled with probability zero so, in expectation, each sample of x is observed with one label y^* (a property of many common image datasets). As such, $z_x = \arg \max_z p_\theta(y^*|z)$, which is independent of x (so renamed z_{y^*}), and all samples x with the same label y have the same optimal $q_\phi(z|x)$. Hence the class level latent distribution is that same delta distribution $q_\phi(z|y) = \delta_{z-z_y}$, meaning that softmax cross entropy loss (for continuous \mathcal{X}) is minimised if all latent representations of a class “collapse” to a point, irrespective of $p_\theta(z|y)$; proving that a softmax classifier may not learn to fit the empirical latent distribution to the class priors anticipated for label predictions.⁴ In practical terms, softmax cross entropy loss aims to map any two samples of a class, regardless of differences in respective probabilities or semantics, to the same point, losing all such information from the representation.

This is remedied if $p_\theta(y|z)$ and $q_\phi(z|y)$ are made *consistent under Bayes' rule*, analogous to $p_\theta(x|z)$ and $q_\phi(z|x)$ in the ELBO (§2). We therefore define $p_\theta(y|z) = \frac{p_\theta(z|y)p_\pi(y)}{\sum_{y'} p_\theta(z|y')p_\pi(y')}$ and encourage $p_\theta(z|y)$ and $q_\phi(z|y)$ to match by minimising $D_{\text{KL}}[q_\phi(z|y) \parallel p_\theta(z|y)]$.

Adding this constraint (weighted by $\beta > 0$) and modelling the class distribution $p_\pi(y)$ gives the full **VC objective**:

³From $p(z|x, y)p(y|x) = p(y|x, z)p(z|x)$ and Markov, we see that $D_{\text{KL}}[q_\phi(z|x) \parallel p_\theta(z|x, y)] = 0 \Leftrightarrow p_\theta(z|x, y) = q_\phi(z|x) \Leftrightarrow p_\theta(y|x) = p_\theta(y|x, z) = p_\theta(y|z) \Leftrightarrow z$ a sufficient statistic for $y|x$.

⁴A less extreme but similar effect occurs for rare items in a discrete domain.

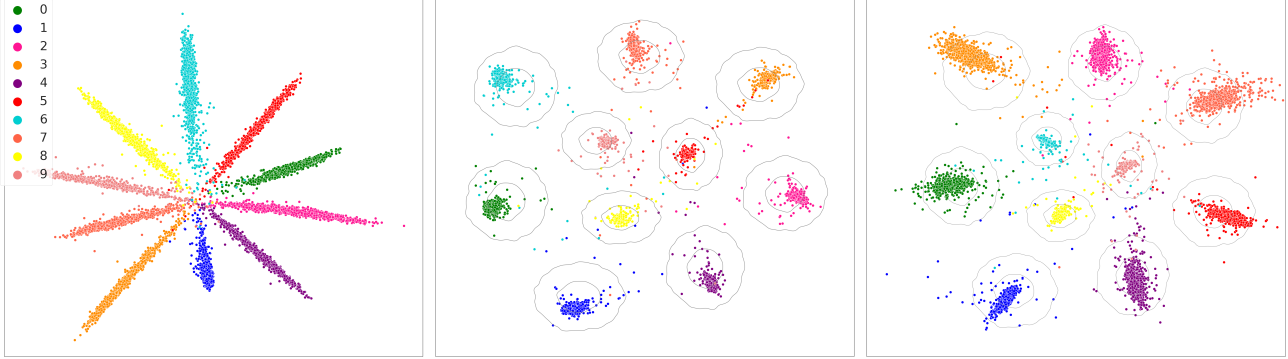


Figure 2: Empirical distributions $q_\phi(z|y)$ for classifiers trained under incremental components of the VC objective (Eq. 7) on MNIST (compares to the central plane in Fig. 1), colour indicates class y : (l) MLE version, equivalent to inputs to the softmax layer trained under cross-entropy; (c) MAP version, MLE + Gaussian class priors $p_\theta(z|y)$ (in contour); and (r) MAP + entropy (i.e. full VC objective). [$\mathcal{Z} = \mathbb{R}^2$ is artificially restricted to 2-D for visualisation.]

$$\max_{\theta, \phi, \pi} \int_{x, y} p(x, y) \left\{ \int_z q_\phi(z|x) \log p_\theta(y|z) - \beta \int_z q_\phi(z|y) \log \frac{q_\phi(z|y)}{p_\theta(z|y)} + \log p_\pi(y) \right\}. \quad (7)$$

Considered incrementally, q_ϕ -terms of the VC objective can be interpreted as treating latent variable z from a *maximum likelihood, maximum a posteriori* and *Bayesian* perspective:

- (i) maximising $\int_z q_\phi(z|x) \log p_\theta(y|z)$ may overfit $q_\phi(z|y)$ to δ_{z-z_y} for finite samples (as above); [MLE]
- (ii) adding *class priors* $\int_z q_\phi(z|y) \log p_\theta(z|y)$ constrains the MLE point estimates z_y [MAP]
- (iii) adding *entropy* $-\int_z q_\phi(z|y) \log q_\phi(z|y)$ encourages $q_\phi(z|y)$ to “fill out” $p_\theta(z|y)$. [Bayesian]

Figure 2 shows samples from empirical latent distributions $q_\phi(z|y)$ for classifiers trained under incremental terms of the VC objective. This demonstrates that the softmax cross entropy loss does not instill the latent distribution anticipated in the last layer (*left*). Adding class priors $p_\theta(z|y)$ induces notable latent structure (*centre*), and adding entropy encourages the priors to be “filled out” (*right*). Despite the MLE/MAP training objectives being optimised when $q_\phi(z|y)$ collapses to a point for datasets where each x occurs with a single label (e.g. MNIST used in Figure 2), we note that this does not occur in practice. We conjecture that this is due to f_ω being both continuous and typically further constrained, e.g. by ℓ_2 regularisation and heuristics such as batch norm.

Comparing to the KL form of the ELBO (Eq. 3), maximising Eq. 7 is equivalent to minimising:

$$\mathbb{E}_x [D_{\text{KL}}[p(y|x) \parallel p_\theta(y|x)]] + \mathbb{E}_{x, y} [D_{\text{KL}}[q_\phi(z|x) \parallel p_\theta(z|x, y)]] + \mathbb{E}_y [D_{\text{KL}}[q_\phi(z|y) \parallel p_\theta(z|y)]] + D_{\text{KL}}[p(y) \parallel p_\pi(y)], \quad (8)$$

which shows the additional constraints over the original objective of modelling $p(y|x)$ by $p_\theta(y|x)$ (in bold). The VC

abstracts a typical neural network classifier giving a simple interpretation of its components:

- the neural network up to the last layer (f_ω) transforms a mixture of analytically unknown class-conditional data distributions $p(x|y)$ to a mixture of analytically defined latent distributions $p_\theta(z|y)$;
- with latent variables following the anticipated mixture of class distributions, label predictions can be “read off” in the last (*generalised softmax*) layer by Bayes’ rule (see Fig. 1).

3.1. Summary of Variational vs Softmax Classification

Having seen that softmax cross entropy loss is a special case of ELBO_{VC} makes clear how it relates to the full VC objective. Variational classification treats the input to the softmax layer as a latent variable and allows the distributional form of $p_\theta(z|y)$ made implicitly within a softmax layer to be generalised to any chosen class prior. More significantly, the VC objective encourages empirical latent distributions $q_\phi(z|y)$ to fit those class priors.

Standard softmax cross entropy loss is recovered from the VC objective under the assumptions $q_\phi(z|x) = \delta_{z-f_\omega(x)}$ ($\forall x \in \mathcal{X}$); class priors $p(z|y)$ are (equal-scale) *exponential family* distributions, e.g. equivariant Gaussians; and $\beta = 0$. A deterministic auto-encoder can be recovered analogously from a variational autoencoder.

Understanding how softmax classification fits within the VC context shows that variational classification does not add complexity by requiring difficult distributional assumptions to be made, rather it elucidates assumptions made implicitly in softmax classification. By generalising the softmax case, variational classification enables assumptions about $p_\theta(z|y)$ to be challenged and changed on a task/data-specific basis.

Algorithm 1 Variational Classification (VC)

Input $p_\theta(z|y), q_\phi(z|x), p_\pi(y), T_\psi(z)$; learning rate schedule $\{\eta_\theta^t, \eta_\phi^t, \eta_\pi^t, \eta_\psi^t\}_t$
 Initialise $\theta, \phi, \pi, \psi; t \leftarrow 0$
while not converged **do**

$\{x_i, y_i\}_{i=1}^m \sim \mathcal{D}$ for $z = \{1 \dots m\}$ do $z_i \sim q_\phi(z x_i), z'_i \sim p_\theta(z y_i)$ $p_\theta(y_i z_i) = \frac{p_\theta(z_i y_i)p_\pi(y_i)}{\sum_y p_\theta(z_i y)p_\pi(y)}$ end for $g_\theta \leftarrow \frac{1}{m} \sum_{i=1}^m \nabla_\theta [\log p_\theta(y_i z_i) + p_\theta(z_i y_i)]$ $g_\phi \leftarrow \frac{1}{m} \sum_{i=1}^m \nabla_\phi [\log p_\theta(y_i z_i) - T_\psi(z_i)]$ $g_\pi \leftarrow \frac{1}{m} \sum_{i=1}^m \nabla_\pi \log p_\pi(y_i)$ $g_\psi \leftarrow \frac{1}{m} \sum_{i=1}^m \nabla_\psi [\log \sigma(T_\psi(z_i)) + \log(1 - \sigma(T_\psi(z'_i)))]$ $\theta \leftarrow \theta + \eta_\theta^t g_\theta, \quad \phi \leftarrow \phi + \eta_\phi^t g_\phi, \quad \pi \leftarrow \pi + \eta_\pi^t g_\pi, \quad \psi \leftarrow \psi + \eta_\psi^t g_\psi, \quad t \leftarrow t + 1$	[sample batch from data distribution $p(x, y)$] [e.g. $q_\phi(z x_i) \doteq \delta_{z-f_\omega(x_i)}, \phi \doteq \omega \Rightarrow z_i = f_\omega(x_i)$] [e.g. using “reparameterisation trick”]
--	--

end while

3.2. Optimising the VC Objective

The VC objective (Eq. 7) is a lower bound that can be maximised by standard gradient-based methods:

- the first term can be calculated by sampling $q_\phi(z|x)$ (using the “reparameterisation trick” if necessary (Kingma & Welling, 2014)) and computing $p_\theta(y|z)$ by Bayes’ rule;
- the third term is standard multinomial cross-entropy;
- the second term, however, is not readily computable since $q_\phi(z|y)$ is defined implicitly and cannot be evaluated, only sampled from by sampling $z \sim q_\phi(z|x)$ (parameterised by f_ω) given $x \sim p(x|y)$.

Fortunately, we require log ratios $\log \frac{q_\phi(z|y)}{p_\theta(z|y)}$ for each class y , which can each be approximated by training a binary classifier to distinguish between samples from $q_\phi(z|y)$ and $p_\theta(z|y)$. This *contrastive* “trick” is increasingly common and underpins learning methods such as Noise Contrastive Estimation (Gutmann & Hyvärinen, 2010), contrastive learning approaches (e.g. Oord et al., 2018) and has been used in a similar way to train variants of the VAE (Makhzani et al., 2015; Mescheder et al., 2017).

Specifically, we maximise the following *auxiliary objective* w.r.t. parameters ψ of a set of binary classifiers:

$$\int_y p(y) \left\{ \int_z q_\phi(z|y) \log \sigma(T_\psi^y(z)) + \int_z p_\theta(z|y) \log(1 - \sigma(T_\psi^y(z))) \right\} \quad (9)$$

where σ is the logistic sigmoid function $\sigma(x) = (1 + e^{-x})^{-1}$, $T_\psi^y(z) = w_y^\top z + b_y$ and $\psi = \{w_y, b_y\}_{y \in \mathcal{Y}}$. It is easy to show that Eq. 9 is optimised if $T_\psi^y(z) = \log \frac{q_\phi(z|y)}{p_\theta(z|y)}$, $\forall y \in \mathcal{Y}$, so that when all binary classifiers are trained, $T_\psi^y(z)$ approximates the log ratio for class y required in the VC objective (Eq. 7). Optimising the VC objective might, in principle, also require gradients of these approximated log

ratios w.r.t parameters θ and ϕ . However, the gradient w.r.t. the ϕ within the log ratio is always zero (Mescheder et al., 2017), and the gradient w.r.t. θ can be computed from Eq. 7. See Algorithm 1 for a summary.

This approach is *adversarial* since: the VC objective is maximised when log ratios are *minimal* (0), whereby $q_\phi(z|y) = p_\theta(z|y)$ and latent samples from the neural network are indistinguishable from those of the prior; whereas the auxiliary objective is maximised if log ratios are *maximal* and the two distributions are optimally discriminated. Similar to a Generative Adversarial Network (GAN) (Goodfellow et al., 2014a), the neural network f_ω can be considered a *generator* and each binary classifier a *discriminator*. Unlike a GAN, VC requires one discriminator per class and each must distinguish generated samples from a learned, not static, reference/noise distribution $p_\theta(z|y)$. However, whereas a GAN discriminator typically distinguishes between complex distributions, a VC discriminator compares a Gaussian to an approximate Gaussian, a far simpler task. The auxiliary objective is parallelised across classes and adds marginal computational overhead per class.

3.3. Optimum of the VC Objective

Having established the form of $q_\phi(z|x)$ that optimises the ELBO_{VC} to better understand softmax classification, the same can be done for variational classification by finding $q_\phi(z|x)$ that maximises the VC objective. We might hope this shows that $q_\phi(z|y)$ learns to fit the prior $p_\theta(z|y)$.

Letting $\beta = 1$ to simplify (generalised in §A.2), it can be seen that the VC objective is maximised w.r.t. $q_\phi(z|x)$ if:

$$\mathbb{E}_{p(y|x)} [\log q_\phi(z|y)] = \mathbb{E}_{p(y|x)} [\log p_\theta(y|z)p_\theta(z|y)] + c, \quad (10)$$

for a constant c . This is satisfied if, for each class y ,

$$q_\phi(z|y) = p_\theta(z|y) \frac{p_\theta(y|z)}{\mathbb{E}_{p_\theta(z'|y)} [p_\theta(y|z')]} , \quad (11)$$

which is a unique solution if each x has only one label y , as discussed above (see §A.2 for a proof). This reveals that empirical distributions $q_\phi(z|y)$ fit class priors $p_\theta(z|y)$ subject to a ratio of $p_\theta(y|z)$ to its weighted average: where $p_\theta(y|z)$ is “above average”, $q_\phi(z|y)$ will exceed $p_\theta(z|y)$, and vice versa. In simple terms, $q_\phi(z|y)$ reflects $p_\theta(z|y)$ but is “peakier”, fitting with observation in Figure 2. This is close to what we set out to achieve and we leave the potential derivation of an objective that simultaneously learns $p_\theta(y|x) = p(y|x)$ and $q_\phi(z|y) = p_\theta(z|y)$ to future work.

4. Related Work

Despite notable differences, the *energy-based* interpretation of softmax classification of Grathwohl et al. (2019) is perhaps most comparable to our own in taking an abstract view of softmax classification to improve aspects of it.. However, their achieved benefits, e.g. to calibration and adversarial robustness, come at a significant cost to the main goal of classification accuracy. Further, the MCMC normalisation required reportedly slows and destabilises training, whereas we use tractable probability distributions and maintain the order of complexity.

Several previous works adapt the standard ELBO, used to learn a model of $p(x)$, to a conditional analog for learning $p(y|x)$ (Tang & Salakhutdinov, 2013; Sohn et al., 2015). However, such works focus on generative scenarios rather than classification, e.g. x being a face image and $y|x$ being the same face in a different pose determined by latent z ; or x being part of an image and $y|x$ its completion given latent content z . The *Gaussian stochastic neural network* (GSNN) model (Sohn et al., 2015) is closer to our own by conditioning $q(z|x, y)$ only on x , however neither model generalises softmax classification or considers class-level latent priors $q(z|y)$ as in variational classification.

Variational classification subsumes many works that add a regularisation term to a softmax cross-entropy loss function, which can be interpreted as a prior over latent variables in the “MAP” case. For example, several semi-supervised learning models can be interpreted as treating the softmax *outputs* as latent variables and using the latent prior to guide the predictions of unlabelled data (Allen et al., 2020). Closer to variational classification, several works can be interpreted as treating softmax *inputs* as latent variables with a regularisation term that encourages prior beliefs, such as *deterministic* label predictions (i.e. all probability mass on a single class), which can be encouraged by imposing a *large margin* between class-conditional latent distributions (Liu et al., 2016; Wen et al., 2016; Wan et al., 2018; 2022).

Variational classification also sits amongst works spanning several learning paradigms in which a Gaussian mixture prior is imposed in the latent space, e.g. for representa-

tion learning (Xie et al., 2016; Caron et al., 2018), in auto-encoders (Song et al., 2013; Ghosh et al., 2019) and in variational auto-encoders (Jiang et al., 2016; Yang et al., 2017; Prasad et al., 2020; Manduchi et al., 2021).

5. Empirical Validation

Our goal is to empirically demonstrate that the latent structure induced by the VC objective is beneficial relative to the standard softmax classifier. A variational classifier can be substituted wherever a softmax classifier is used, by making distributional choices appropriate for the data. In particular, variational classification does not set out to address any one drawback of a softmax classifier, rather it aims to better reverse the generative process and so capture the data distribution, providing multiple benefits. We illustrate the effectiveness of a VC through a variety of tasks on familiar datasets from the visual and text domains. Specifically, we set out to validate the following hypotheses:

- H1:** The VC objective improves uncertainty estimation, leading to a more calibrated model.
- H2:** The VC objective increases model robustness to changes in the data distribution.
- H3:** The VC objective enhances resistance to adversarial perturbations.
- H4:** The VC objective aids learning from fewer samples.

For a fair comparison, we make minimal changes to adapt a standard softmax classifier to a variational classifier. As described in §3.1, we train with the VC objective (equation 7) under the following assumptions: $q_\phi(z|x)$ is a delta distribution parameterised by a neural network $f_\omega : \mathcal{X} \rightarrow \mathcal{Z}$; class-conditional priors $p_\theta(z|y)$ are multi-variate Gaussians with parameters learned from the data (we use diagonal covariance for simplicity). To provide an ablation across the components of the VC objective, we compare classifiers trained to maximise three objective functions (see §3):

CE: equivalent to standard softmax cross-entropy under the above assumptions and corresponds to the MLE form of the VC objective (§2, (i)).

$$J_{\text{CE}} = \int_{x,y} p(x,y) \{ \int_z q_\phi(z|x) \log p_\theta(y|z) + \log p_\pi(y) \}$$

GM: includes class priors and corresponds to the MAP form of the VC objective (§2, (ii)).

$$J_{\text{GM}} = J_{\text{CE}} + \int_{x,y} p(x,y) \int_z q_\phi(z|y) \log p_\theta(z|y)$$

VC: includes entropy of the empirical latent distributions and corresponds to the Bayesian form of the VC objective (§2, (iii)).

$$J_{\text{VC}} = J_{\text{GM}} - \int_{x,y} p(x,y) \int_z q_\phi(z|y) \log q_\phi(z|y)$$

	CIFAR-10			CIFAR-100				TINY-IMAGENET		
	CE	GM	VC	CE	GM	VC	JEM	CE	GM	VC
<i>Accuracy (% , \uparrow)</i>										
WRN	96.2 ± 0.1	95.0 ± 0.2	96.3 ± 0.2	80.3 ± 0.1	79.8 ± 0.2	80.3 ± 0.1	72.2^*	-	-	-
RNET	93.7 ± 0.1	93.0 ± 0.1	93.2 ± 0.1	73.2 ± 0.1	74.2 ± 0.1	73.4 ± 0.1	-	59.7 ± 0.2	59.3 ± 0.1	59.3 ± 0.1
<i>Calibration (% , \downarrow)</i>										
WRN	3.1 ± 0.2	3.5 ± 0.3	2.1 ± 0.2	11.1 ± 0.7	19.6 ± 0.4	4.8 ± 0.3	4.9^*	-	-	-
RNET	3.8 ± 0.3	4.1 ± 0.2	3.2 ± 0.2	8.7 ± 0.2	10.5 ± 0.2	5.1 ± 0.2	-	12.3 ± 0.4	8.75 ± 0.2	7.4 ± 0.5

Table 1: Classification Accuracy and Expected Calibration Error (mean and std.dev. over 5 runs). Accuracy remains comparable across all VC-based models and data sets; calibration varies materially. *results from original paper

5.1. Accuracy and Calibration

We first compare the classification accuracy and calibration of each model on three standard benchmarks (CIFAR-10, CIFAR-100, and TINY-IMAGENET), across two standard ResNet model architectures (*WideResNet-28-10* (WRN) and *ResNet-50* (RNET)) (He et al., 2016; Zagoruyko & Komodakis, 2016). Calibration is evaluated in terms of the *Expected Calibration Error* (ECE) (see Appendix C).

Table 1 shows that the VC and GM models achieve comparable accuracy to softmax cross entropy (CE), but that the VC model is consistently, significantly more calibrated (**H1**). Unlike approaches such as Platt’s scaling (Platt et al., 1999) and temperature scaling (Guo et al., 2017), no *post hoc* calibration is performed, no external calibration set is needed or calibration-specific hyperparameters tuned.

5.2. Generalization under distribution shift

When used in real-world settings, machine learning models may encounter *distribution shift* relative to the training data. It can be important to know when a model’s output is reliable and can be trusted, requiring the model to be **calibrated on out-of-distribution (OOD) data** and *know when they do not know*. To test performance under distribution shift, we use the robustness benchmarks, CIFAR-10-C, CIFAR-100-C and TINY-IMAGENET-C, proposed by Hendrycks & Dietterich (2019), which *simulate* distribution shift by adding various corruptions of varying intensities to a dataset. We compare the CE model, with and without temperature scaling, to the VC model. Temperature scaling was performed as in Guo et al. (2017) with the temperature tuned on an in-distribution validation set.

Both models are found to perform comparably in terms of classification accuracy (Figure 7), according to previous results (§5.1). However, Figure 3 shows that the VC model has a consistently lower calibration error as the corruption intensity increases (left to right) (**H2**). We note that the improvement in calibration between the CE and VC models increases as the complexity of the dataset increases.

When deployed in the wild, *natural* distributional shifts may occur in the data due to subtle changes in the data generation process, e.g. a change of camera. We test re-

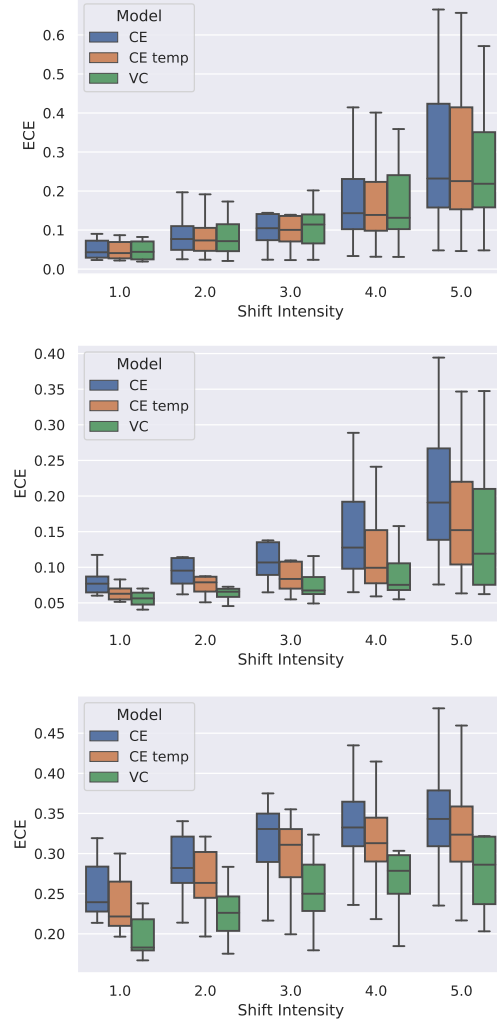


Figure 3: Calibration under distribution shift: boxes indicate quartiles summarizing results across 16 shift types, whiskers indicate min/max across shift types. (top) CIFAR-10-C, (middle) CIFAR-100-C, (bottom) TINY-IMAGENET-C

silence to natural distributional shifts on two tasks: Natural Language Inference (NLI) and detecting whether cells are cancerous from microscopic images. NLI requires verifying if a hypothesis logically follows from a premise. Models are trained on the SNLI dataset (Bowman et al., 2015) and tested on the MNLI dataset (Williams et al., 2018) taken from more

diverse sources. Cancer detection uses the CAMELYON17 dataset (Bandi et al., 2018) from the WILDS datasets (Koh et al., 2021), where the `train` and `eval` sets contain images from different hospitals.

Table 2 shows that the VC model achieves better calibration under these natural distributional shifts (**H2**). The CAMELYON17 dataset has a relatively small number (1000) of training samples (hence wide error bars are expected), which combines distribution shift with a low data setting (**H4**) and shows that the VC model achieves higher (average) accuracy in this more challenging real-world setting.

We also test the ability to **detect OOD examples**. We compute the AUROC when a model is trained on CIFAR-10 and evaluated on the CIFAR-10 validation set mixed (in turn) with SVHN, CIFAR-100, and CELEBA (Goodfellow et al., 2013; Liu et al., 2015). We compare the VC and CE models using the probability of the predicted class $\arg \max_y p_\theta(y|x)$ as a means of identifying OOD samples.

Table 3 shows that the VC model performs comparably to the CE model. We also consider $p(z)$ as a metric to detect OOD samples and again achieve comparable results, which is broadly consistent with the findings of Grathwohl et al. (2019). Although the VC model learns to map the data to a more structured latent space and, from the results above, makes more calibrated predictions for OOD data, it does not appear to be better able to distinguish OOD data than a standard softmax classifier (CE) using the metrics tested (we note that ‘‘OOD’’ is a very loosely defined term).

5.3. Adversarial Robustness

We test model robustness by measuring performance on adversarially generated images using the common *Fast Gradient Sign Method* (FGSM) of adversarial attack (Good-

	Accuracy (\uparrow)		Calibration (\downarrow)	
	CE	VC	CE	VC
NLI	71.2 \pm 0.1	71.2 \pm 0.1	7.3 \pm 0.2	3.4 \pm 0.2
CAMELYON17	79.2 \pm 2.8	84.5 \pm 4.0	8.4 \pm 2.5	1.8 \pm 1.3

Table 2: Accuracy and ECE under distributional shift (mean and std. err over 5 runs)

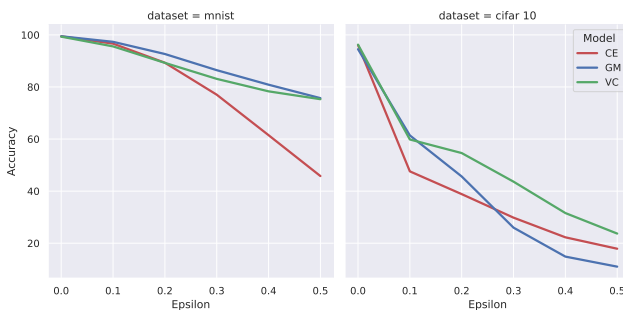


Figure 4: Prediction accuracy as FGSM adversarial attacks increase (*l*) MNIST; (*r*) CIFAR-10

Model	SVHN	C-100	CelebA
$P_{CE}(y x)$	0.92	0.88	0.90
$P_{VC}(y z)$	0.93	0.86	0.89

Table 3: AUROC for the OOD detection task. Models are trained on CIFAR-10 and evaluated on in and out-of-distribution samples.

	CE	GM	VC
MNIST	93.1 \pm 0.2	94.4 \pm 0.1	94.2 \pm 0.2
CIFAR-10	52.7 \pm 0.5	54.2 \pm 0.6	56.3 \pm 0.6
AGNEWS	49.2 \pm 0.5	50.8 \pm 0.5	51.3 \pm 0.4

Table 4: Low data accuracy (mean and std err on 5 runs)

fellow et al., 2014b). Perturbations are generated as $P = \epsilon \times \text{sign}(\mathcal{L}(x, y))$, where $\mathcal{L}(x, y)$ is the model loss for data sample x and correct class y ; and ϵ is the *magnitude* of the attack. We compare all models trained on MNIST and CIFAR-10 against FGSM attacks of different magnitudes.

Results in Figure 4 show that the VC model is consistently more adversarially robust relative to the standard CE model, across attack magnitudes on both datasets (**H3**).

5.4. Low Data Regime

Lastly, we investigate model performance when data is scarce on the hypothesis that a prior over the latent space may allow a model to generalise better from fewer samples. Models are trained on 500 samples from MNIST, 1000 samples from CIFAR-10 and 50 samples from AGNEWS.

Results in Table 4 show that introducing the prior (GM) improves performance in a low data regime and that the additional entropy term in the VC model maintains or further improves accuracy (**H4**), particularly on the more complex datasets.

6. Conclusion

We have presented Variational Classification (VC), a generalisation of the softmax classifier, mirroring the relationship between the variational auto-encoder and the deterministic auto-encoder (§3). We show that the softmax classifier is a special case of a VC under specific assumptions that are effectively taken for granted when using the softmax output layer. We present a training objective to train a VC analogous to the ELBO, together with an adversarial optimisation regime. A series of experiments on image and text datasets show that, with marginal computational overhead and without tuning hyper-parameters other than for the original classification task, a variational classifier achieves comparable classification accuracy to standard softmax while outperforming in terms of calibration, adversarial robustness and under distribution shift or in low data settings (§5).

In terms of limitations, we focus largely on the output layer

of a softmax classifier, treating the function beneath, f_ω , as a “black-box”. This leaves an open question: what does, or should, the rest of the network do? We also show that empirical latent distributions $q_\phi(z|y)$ learn a “peaky” approximation to the anticipated class priors $p_\theta(z|y)$, suggesting possible scope for improvement to the VC objective (§3.3).

The VC model gives new theoretical insight into the highly familiar softmax classifier, opening up several interesting future directions. For example, $q(z|x)$ might be modelled as a stochastic distribution rather than a delta function to reflect uncertainty in the latent variables. It may also be extended to semi-supervised learning similar to other methods that implicitly impose a prior in the latent space.

References

Adem, K., Kılıçarslan, S., and Cömert, O. Classification and diagnosis of cervical cancer with stacked autoencoder and softmax classification. *Expert Systems with Applications*, 115:557–564, 2019.

Allen, C., Balažević, I., and Hospedales, T. A probabilistic model for discriminative and neuro-symbolic semi-supervised learning. *arXiv preprint arXiv:2006.05896*, 2020.

Bandi, P., Geessink, O., Manson, Q., Van Dijk, M., Balkenhol, M., Hermsen, M., Bejnordi, B. E., Lee, B., Paeng, K., Zhong, A., et al. From detection of individual metastases to classification of lymph node status at the patient level: the camelyon17 challenge. *IEEE Transactions on Medical Imaging*, 2018.

Bowman, S. R., Angeli, G., Potts, C., and Manning, C. D. A large annotated corpus for learning natural language inference. *arXiv preprint arXiv:1508.05326*, 2015.

Caron, M., Bojanowski, P., Joulin, A., and Douze, M. Deep clustering for unsupervised learning of visual features. In *Proceedings of the European conference on computer vision (ECCV)*, pp. 132–149, 2018.

Ghosh, P., Sajjadi, M. S., Vergari, A., Black, M., and Schölkopf, B. From variational to deterministic autoencoders. *arXiv preprint arXiv:1903.12436*, 2019.

Goodfellow, I. J., Bulatov, Y., Ibarz, J., Arnoud, S., and Shet, V. Multi-digit number recognition from street view imagery using deep convolutional neural networks. *arXiv preprint arXiv:1312.6082*, 2013.

Goodfellow, I. J., Pouget-Abadie, J., Mirza, M., Xu, B., Warde-Farley, D., Ozair, S., Courville, A. C., and Bengio, Y. Generative adversarial nets. In *NIPS*, 2014a.

Goodfellow, I. J., Shlens, J., and Szegedy, C. Explaining and harnessing adversarial examples. *arXiv preprint arXiv:1412.6572*, 2014b.

Grathwohl, W., Wang, K.-C., Jacobsen, J.-H., Duvenaud, D., Norouzi, M., and Swersky, K. Your classifier is secretly an energy based model and you should treat it like one. In *International Conference on Learning Representations*, 2019.

Guo, C., Pleiss, G., Sun, Y., and Weinberger, K. Q. On calibration of modern neural networks. In *International conference on machine learning*, pp. 1321–1330. PMLR, 2017.

Gutmann, M. and Hyvärinen, A. Noise-contrastive estimation: A new estimation principle for unnormalized statistical models. In *Proceedings of the thirteenth international conference on artificial intelligence and statistics*, pp. 297–304. JMLR Workshop and Conference Proceedings, 2010.

He, K., Zhang, X., Ren, S., and Sun, J. Deep residual learning for image recognition. In *Proceedings of the IEEE conference on computer vision and pattern recognition*, pp. 770–778, 2016.

Hendrycks, D. and Dietterich, T. Benchmarking neural network robustness to common corruptions and perturbations. *arXiv preprint arXiv:1903.12261*, 2019.

Jiang, Z., Zheng, Y., Tan, H., Tang, B., and Zhou, H. Variational deep embedding: An unsupervised and generative approach to clustering. *arXiv preprint arXiv:1611.05148*, 2016.

Kingma, D. P. and Welling, M. Auto-encoding variational bayes. *International Conference on Learning Representations*, 2014.

Klasson, M., Zhang, C., and Kjellström, H. A hierarchical grocery store image dataset with visual and semantic labels. In *IEEE Winter Conference on Applications of Computer Vision (WACV)*, 2019.

Koh, P. W., Sagawa, S., Marklund, H., Xie, S. M., Zhang, M., Balsubramani, A., Hu, W., Yasunaga, M., Phillips, R. L., Gao, I., et al. Wilds: A benchmark of in-the-wild distribution shifts. In *International Conference on Machine Learning*, pp. 5637–5664. PMLR, 2021.

Liu, W., Wen, Y., Yu, Z., and Yang, M. Large-margin softmax loss for convolutional neural networks. In *International Conference on Machine Learning*, 2016.

Liu, Z., Luo, P., Wang, X., and Tang, X. Deep learning face attributes in the wild. In *Proceedings of International Conference on Computer Vision (ICCV)*, December 2015.

Makhzani, A., Shlens, J., Jaitly, N., Goodfellow, I., and Frey, B. Adversarial autoencoders. *arXiv preprint arXiv:1511.05644*, 2015.

Manduchi, L., Chin-Cheong, K., Michel, H., Wellmann, S., and Vogt, J. Deep conditional gaussian mixture model for constrained clustering. *Advances in Neural Information Processing Systems*, 34:11303–11314, 2021.

Mescheder, L., Nowozin, S., and Geiger, A. Adversarial variational bayes: Unifying variational autoencoders and generative adversarial networks. In *International conference on machine learning*, pp. 2391–2400. PMLR, 2017.

Mirbabaie, M., Stieglitz, S., and Frick, N. R. Artificial intelligence in disease diagnostics: A critical review and classification on the current state of research guiding

future direction. *Health and Technology*, 11(4):693–731, 2021.

Mukhoti, J., Kirsch, A., van Amersfoort, J., Torr, P. H., and Gal, Y. Deep deterministic uncertainty: A simple baseline. *arXiv e-prints*, pp. arXiv–2102, 2021.

Naeini, M. P., Cooper, G., and Hauskrecht, M. Obtaining well calibrated probabilities using bayesian binning. In *Twenty-Ninth AAAI Conference on Artificial Intelligence*, 2015.

Oord, A. v. d., Li, Y., and Vinyals, O. Representation learning with contrastive predictive coding. *arXiv preprint arXiv:1807.03748*, 2018.

Platt, J. et al. Probabilistic outputs for support vector machines and comparisons to regularized likelihood methods. *Advances in large margin classifiers*, 10(3):61–74, 1999.

Prasad, V., Das, D., and Bhowmick, B. Variational clustering: Leveraging variational autoencoders for image clustering. In *2020 international joint conference on neural networks (IJCNN)*, pp. 1–10. IEEE, 2020.

Rezende, D. J., Mohamed, S., and Wierstra, D. Stochastic backpropagation and approximate inference in deep generative models. In *International conference on machine learning*, 2014.

Sohn, K., Lee, H., and Yan, X. Learning structured output representation using deep conditional generative models. *Advances in neural information processing systems*, 28, 2015.

Song, C., Liu, F., Huang, Y., Wang, L., and Tan, T. Autoencoder based data clustering. In *Iberoamerican congress on pattern recognition*, pp. 117–124. Springer, 2013.

Tang, C. and Salakhutdinov, R. R. Learning stochastic feed-forward neural networks. *Advances in Neural Information Processing Systems*, 2013.

Tiensuu, J., Linderholm, M., Dreborg, S., and Örn, F. Detecting exoplanets with machine learning: A comparative study between convolutional neural networks and support vector machines, 2019.

Wan, W., Zhong, Y., Li, T., and Chen, J. Rethinking feature distribution for loss functions in image classification. In *Proceedings of the IEEE conference on computer vision and pattern recognition*, pp. 9117–9126, 2018.

Wan, W., Chen, J., Yu, C., Wu, T., Zhong, Y., and Yang, M.-H. Shaping deep feature space towards gaussian mixture for visual classification. *IEEE Transactions on Pattern Analysis and Machine Intelligence*, 2022.

Wen, Y., Zhang, K., Li, Z., and Qiao, Y. A discriminative feature learning approach for deep face recognition. In *European conference on computer vision*, pp. 499–515. Springer, 2016.

Williams, A., Nangia, N., and Bowman, S. A broad-coverage challenge corpus for sentence understanding through inference. In *Proceedings of the 2018 Conference of the North American Chapter of the Association for Computational Linguistics: Human Language Technologies, Volume 1 (Long Papers)*, pp. 1112–1122. Association for Computational Linguistics, 2018. URL <http://aclweb.org/anthology/N18-1101>.

Xie, J., Girshick, R., and Farhadi, A. Unsupervised deep embedding for clustering analysis. In *International conference on machine learning*, pp. 478–487. PMLR, 2016.

Yang, B., Fu, X., Sidiropoulos, N. D., and Hong, M. Towards k-means-friendly spaces: Simultaneous deep learning and clustering. In *international conference on machine learning*, pp. 3861–3870. PMLR, 2017.

Zagoruyko, S. and Komodakis, N. Wide residual networks. *arXiv preprint arXiv:1605.07146*, 2016.

A. Proofs

A.1. Optising the ELBO_{VC} w.r.t q

Rearranging Equation 5, the ELBO_{VC} is optimised by

$$\begin{aligned} & \arg \max_{q_\phi(z|x)} \int_x \sum_y p(x, y) \int_z q_\phi(z|x) \log p_\theta(y|z) \\ &= \arg \max_{q_\phi(z|x)} \int_x p(x) \int_z q_\phi(z|x) \sum_y p(y|x) \log p_\theta(y|z) \end{aligned}$$

Each integral over z is a weighted sum of $\sum_y p(y|x) \log p_\theta(y|z)$ terms, where $q_\phi(z|x)$ weights those terms. Since $q_\phi(z|x)$ is a probability distribution, each integral is upper bounded by $\max_z \sum_y p(y|x) \log p_\theta(y|z)$, which is attained if and only if the support of $q_\phi(z|x)$ falls only on $z^* = \arg \max_z \sum_y p(y|x) \log p_\theta(y|z)$ (which may not be unique). \square

A.2. Optimising the VC objective w.r.t. q

Setting $\beta = 1$ in Equation 7 to simplify and adding a lagrangian term to constrain $q_\phi(z|x)$ to a probability distribution, we aim to find

$$\begin{aligned} & \arg \max_{q_\phi(z|x)} \int_x \sum_y p(x, y) \left\{ \int_z q_\phi(z|x) \log p_\theta(y|z) \right. \\ & \quad \left. - \int_z q_\phi(z|y) \log \frac{q_\phi(z|y)}{p_\theta(z|y)} + \log p_\pi(y) \right\} + \lambda \left(1 - \int_z q_\phi(z|x) \right). \end{aligned}$$

Recalling that $q_\phi(z|y) = \int_x q_\phi(z|x)p(x|y)$ and using calculus of variations, we set the derivative of this functional w.r.t. $q_\phi(z|x)$ to zero

$$\sum_y p(x, y) \left\{ \log p_\theta(y|z) - \left(\log \frac{q_\phi(z|y)}{p_\theta(z|y)} + 1 \right) \right\} - \lambda = 0$$

Rearranging and diving through by $p(x)$ gives

$$\mathbb{E}_{p(y|x)} [\log q_\phi(z|y)] = \mathbb{E}_{p(y|x)} [\log p_\theta(y|z)p_\theta(z|y)] + c,$$

where $c = -(1 + \frac{\lambda}{p(x)})$. Further, if each label y occurs once with each x , due to sampling or otherwise, then this simplifies to

$$q_\phi(z|y^*)e^c = p_\theta(y^*|z)p_\theta(z|y^*),$$

which holds for all classes $y \in \mathcal{Y}$. Integrating over z shows $e^c = \int_z p_\theta(y|z)p_\theta(z|y)$ to give

$$q_\phi(z|y) = \frac{p_\theta(y|z)p_\theta(z|y)}{\int_z p_\theta(y|z)p_\theta(z|y)} = p_\theta(z|y) \frac{p_\theta(y|z)}{\mathbb{E}_{p_\theta(z|y)} [p_\theta(y|z)]}. \quad \square$$

We note, it is straightforward to include β to show

$$q_\phi(z|y) = p_\theta(z|y) \frac{p_\theta(y|z)^{1/\beta}}{\mathbb{E}_{p_\theta(z|y)} [p_\theta(y|z)^{1/\beta}]}.$$

B. Justifying the Latent Prior in Variational Classification

Choosing Gaussian class priors in Variational classification can be interpreted in two ways:

Well-specified generative model: Assume data $x \in \mathcal{X}$ is generated from the hierarchical model: $y \rightarrow z \rightarrow x$, where $p(y)$ is categorical; $p(z|y)$ are analytically known distributions, e.g. $\mathcal{N}(z; \mu_y, \Sigma_y)$; the dimensionality of z is not large; and $x = h(z)$ for an arbitrary invertible function $h: \mathcal{Z} \rightarrow \mathcal{X}$ (if \mathcal{X} is of higher dimension than \mathcal{Z} , assume h maps one-to-one to a manifold in \mathcal{X}). Accordingly, $p(x)$ is a mixture of unknown distributions. If $\{p_\theta(z|y)\}_\theta$ includes the true distribution $p(z|y)$, variational classification effectively aims to invert h and learn the parameters of the true generative model. In practice, the model parameters and h^{-1} may only be identifiable up to some equivalence, but by reflecting the true latent variables, the learned latent variables should be semantically meaningful.

Miss-specified model: Assume data is generated as above, but with z having a large, potentially uncountable, dimension with complex dependencies, e.g. details of every blade of grass or strand of hair in an image. In general, it is impossible to learn all such latent variables with a lower dimensional model. The latent variables of a VC might learn a complex function of multiple true latent variables.

The first scenario is ideal since the model might learn disentangled, semantically meaningful features of the data. However, it requires distributions to be well-specified and a low number of true latent variables. For natural data with many latent variables, the second case seems more plausible but choosing $p_\theta(z|y)$ to be Gaussian may nevertheless be justifiable by the Central Limit Theorem.

C. Calibration Metrics

One way to measure if a model is calibrated is to compute the expected difference between the confidence and expected accuracy of a model.

$$\mathbb{E}_{P(\hat{y}|x)} \left[\mathbb{P}(\hat{y} = y | P(\hat{y}|x) = p) - p \right] \quad (12)$$

This is known as expected calibration error (ECE) (Naeini et al., 2015). Practically, ECE is estimated by sorting the predictions by their confidence scores, partitioning the predictions in M equally spaced bins ($B_1 \dots B_M$) and taking the weighted average of the difference between the average accuracy and average confidence of the bins. In our experiments we use 20 equally spaced bins.

$$\text{ECE} = \sum_{m=1}^M \frac{|B_m|}{n} |acc(B_m) - conf(B_m)| \quad (13)$$

D. OOD Detection

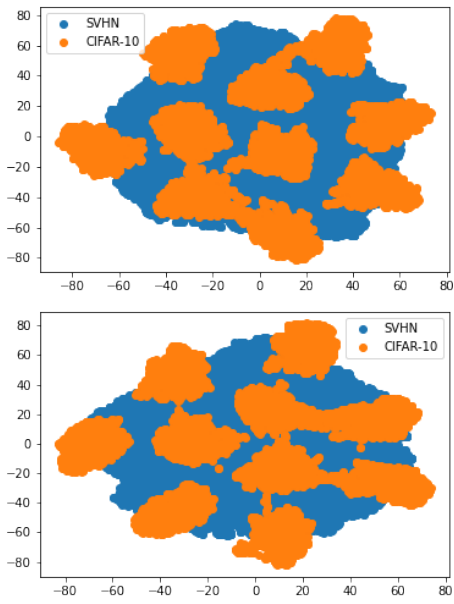


Figure 5: t-SNE plots of the feature space for a classifier trained on CIFAR-10. (l) Trained using CE. (r) Trained using VC. We posit that similar to CE, VC model is unable to meaningfully represent data from an entirely different distribution.

E. Semantics of the latent space

To try to understand the semantics captured in the latent space, we use a pre-trained MNIST model on the *Ambiguous* MNIST dataset (Mukhoti et al., 2021). We interpolate between ambiguous 7's that are mapped close to the Gaussian clusters of classes of “1” and “2”. It can be observed that traversing from the mean of the “7” Gaussian to that on the “1” class, the ambiguous 7's begin to look more like “1”s.

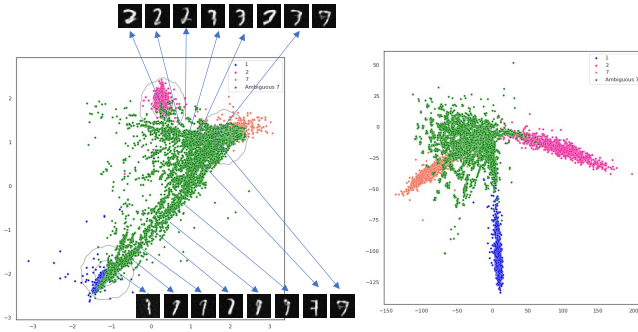


Figure 6: Interpolating in the latent space: Ambiguous MNIST when mapped on the latent space. (l) VC, (r) CE

F. Classification under Domain Shift

A comparison of accuracy between the VC and CE models under 16 different synthetic domain shifts. We find that VC performs comparably well as CE.

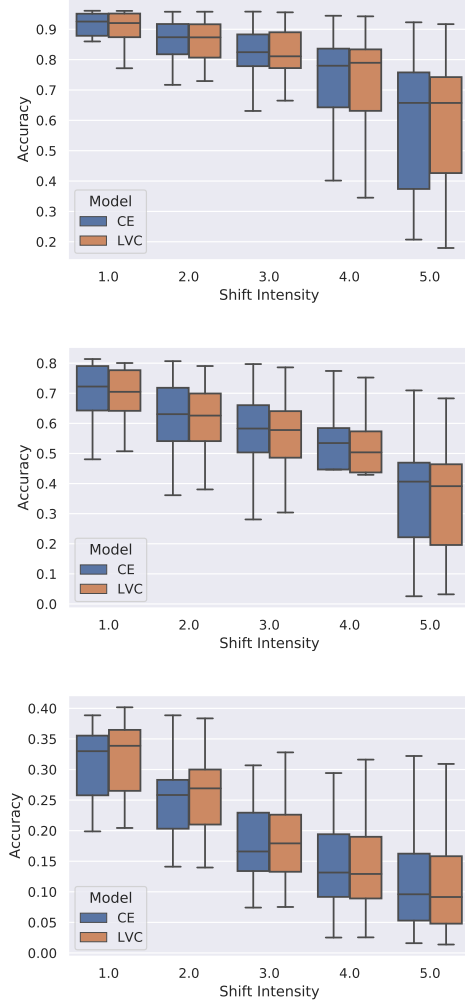


Figure 7: Classification accuracy under distributional shift: (a) CIFAR-10-C (b) CIFAR-100-C (c) TINY-IMAGENET-C